Human Molecular Genetics, 2009, Vol. 18, No. 13 **2359–2369**
doi:10.1093/hmg/ddp168
Advance Access published on April 4, 2009

Thin filament length dysregulation contributes to muscle weakness in nemaline myopathy patients with nebulin deficiency

Coen A.C. Ottenheijm[1,2], Christian C. Witt[3], Ger J. Stienen[2], Siegfried Labeit[3], Alan H. Beggs[4] and Henk Granzier[1,*]

[1]Department of Molecular and Cellular Biology, University of Arizona, Tucson, AZ 85724, USA, [2]Laboratory for Physiology, Institute for Cardiovascular Research, VU University Medical Center, Amsterdam 1081 BT, The Netherlands, [3]Institute for Integrative Pathophysiology, University Hospital Mannheim, Mannheim 68131, Germany and [4]Division of Genetics and Program in Genomics, The Manton Center for Orphan Disease Research, Children's Hospital Boston, Harvard Medical School, Boston, MA 02115, USA

Received January 22, 2009; Revised March 18, 2009; Accepted April 2, 2009

Nemaline myopathy (NM) is the most common non-dystrophic congenital myopathy. Clinically the most important feature of NM is muscle weakness; however, the mechanisms underlying this weakness are poorly understood. Here, we studied the muscular phenotype of NM patients with a well-defined nebulin mutation (NM-NEB), using a multidisciplinary approach to study thin filament length regulation and muscle contractile performance. SDS–PAGE and western blotting revealed greatly reduced nebulin levels in skeletal muscle of NM-NEB patients, with the most prominent reduction at nebulin's N-terminal end. Muscle mechanical studies indicated ~60% reduced force generating capacity of NM-NEB muscle and a leftward-shift of the force–sarcomere length relation in NM-NEB muscle fibers. This indicates that the mechanism for the force reduction is likely to include shorter and non-uniform thin filament lengths in NM-NEB muscle compared with control muscle. Immunofluorescence confocal microscopy and electron microscopy studies indicated that average thin filament length is reduced from ~1.3 μm in control muscle to ~0.75 μm in NM-NEB muscle. Thus, the present study is the first to show a distinct genotype-functional phenotype correlation in patients with NM due to a nebulin mutation, and provides evidence for the notion that dysregulated thin filament length contributes to muscle weakness in NM patients with nebulin mutations. Furthermore, a striking similarity between the contractile and structural phenotypes of nebulin-deficient mouse muscle and human NM-NEB muscle was observed, indicating that the nebulin knockout model is well suited for elucidating the functional basis of muscle weakness in NM and for the development of treatment strategies.

INTRODUCTION

Nemaline myopathy (NM), the most common non-dystrophic congenital myopathy in humans, is characterized at the muscle's ultrastructural level by nemaline rod-like bodies that are composed of thin filament and Z-disk proteins (1). Clinically the most important feature is muscle weakness; however, the mechanisms underlying this weakness are poorly understood.

Six genes have been implicated in NM, all coding for thin filament proteins: *ACTA1* (actin), *TPM3* and *TPM2* (α and β tropomyosin), *TNNT1* (troponinT), *CFL2* (cofilin-2) (2) and *NEB* (nebulin), for a review see Sanoudou and Beggs (3). Hence, NM can be considered a thin filament myopathy. The main form of NM, likely accounting for ~50% of all NM cases, results from mutations in the nebulin gene (4). Nebulin is a giant protein (MW ~800 kDa) expressed at high levels in skeletal muscle. A single nebulin molecule spans the entire thin filament with its C-terminus anchored at the Z-disk and its N-terminal region directed towards the thin filament pointed end (5). Accordingly, nebulin can be considered as a fourth filament system of the sarcomere (after thin, thick and titin filaments, Fig. 1). Recently,

*To whom correspondence should be addressed. Tel: +1 5206263641; Fax: +1 5206267600; Email: granzier@email.arizona.edu

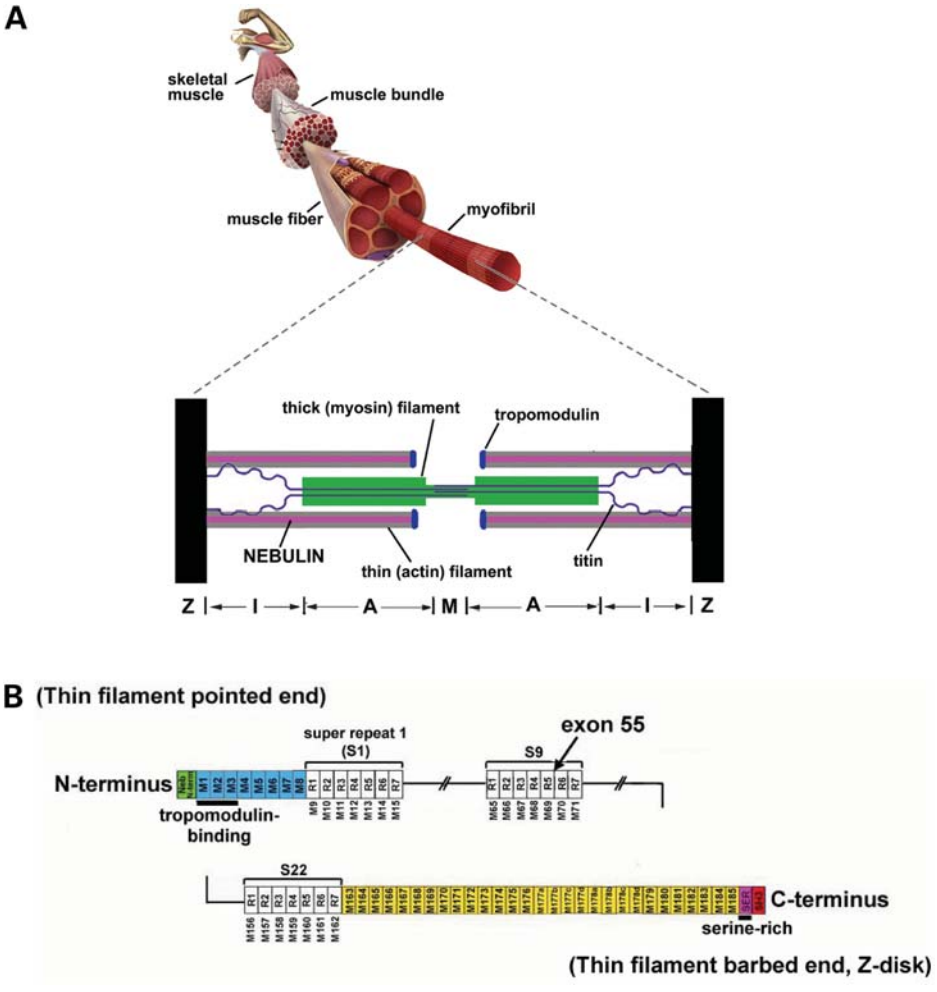

Figure 1. (**A**) Schematic of a skeletal muscle sarcomere. (**B**) Schematic of the human nebulin sequence. Nebulin has a highly modular structure, within the central region (M9-M162) seven modular repeats arranged into twenty-two super-repeats. Exon 55 codes for 35 amino acids that are part of repeat 5 and 6 (super-repeat 9).

using a nebulin knockout mouse model, evidence has been presented that in the absence of nebulin, thin filaments are shorter and might vary in length depending on muscle loading (6,7). Thus, it has been proposed that a nebulin-independent mechanism may specify uniform (but significantly shorter) thin filament lengths in nebulin-deficient myofibrils, but that upon muscle loading nebulin is required to maintain uniform thin filament lengths (8).

Thin filament length is an important determinant of muscle function, because the degree of overlap between thick and thin filaments determines the amount of force that a muscle develops (9); high overlap allows more cross-bridges to interact with the thin filament, and thus more force to be generated. In nebulin-deficient mouse muscle, the thin filaments are on average shorter than in *wt* skeletal muscle, thereby significantly depressing force generation (6,7).

Recent structural and functional studies on murine models with nebulin deficiencies (5,6) stimulated us to investigate the contractile properties of myofibrils from NM patients. In particular, we studied the muscular phenotype of five NM patients with a well-defined nebulin mutation (i.e. deletion of exon 55, resulting in a partial nebulin deficiency), using a multidisciplinary approach to study thin filament length regulation and muscle contractile performance. A side-by-side comparison of NM muscle and nebulin-free mouse muscle shows remarkable phenotypic similarities, i.e. shorter and non-uniform thin filament lengths and significantly impaired force generating capacity. Thus, loss of thin filament length regulation appears to be an important contributor to muscle weakness in patients with NM that have a partial nebulin deficiency.

RESULTS

Nebulin protein levels in NM-NEB patients and controls

We studied skeletal muscle of NM patients in which a small exon relatively close to nebulin's N-terminus (exon 55) was deleted (for patient characteristics, see Table 1). All five patients, two brothers and three other unrelated probands, carry identical deletions as described previously (10). We refer to these patients as NM-NEB patients. The exon 55 deletion maintains nebulin's reading frame which is consistent

Table 1. Human subject and skeletal muscle biopsy characteristics

Patient ID[a]	Genetic status	Gender	Biopsy location	Age at biopsy (years)	Clinical form[b]	Age of onset	Maximal motor ability
na	Unaffected	M	Quad	9.3	—	—	Normal
na	Unaffected	M	Quad	32	—	—	Normal
na	Unaffected	M	Quad	45	—	—	Normal
na	Unaffected	M	Quad	45	—	—	Normal
2–1	*NEB* del e55	M	Rectus abdominis	0.3	Severe	Birth	Never walked
5	*NEB* del e55	F	Quad	0.7	Intermediate	Birth	Used walker at 7
4	*NEB* del e55	F	Quad	1.1	Intermediate	Birth	Never walked
1–2	*NEB* del e55	M	Para-spinal	5.7	Severe	Birth	Never walked
1–1	*NEB* del e55	M	Para-spinal	15.8	Severe	Birth	Used walker at 5

[a]From Lehtokari *et al*. (10).
[b]Clinical form of NM as defined in Sanoudou and Beggs (3).

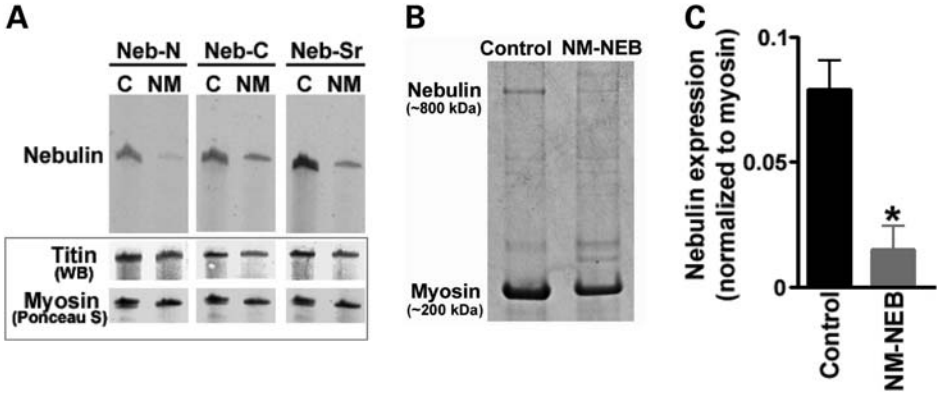

Figure 2. (**A**) Western blotting studies with antibodies against nebulin's N-terminus (Neb-N), C-terminus (Neb-C) and serine-rich domain (Neb-Sr). Nebulin expression is reduced in NM-NEB muscle, with the most severe reduction at the N-terminal end. Bottom: titin and myosin loading controls. (**B** and **C**) SDS–PAGE revealed approximately 8-fold reduced nebulin expression (normalized to myosin) in NM-NEB muscle.

with western blot studies that demonstrated inclusion of nebulin's C-terminal epitopes in NM-NEB muscle extracts [see Fig. 2A (Neb-C and Neb-Ser rich)]. Interestingly, antibodies to nebulin's N-terminus were comparatively less reactive than those to nebulin's C-terminus or serine-rich domain (Fig. 2A). Because exon 55 is part of an actin-binding super-repeat (11–13), its excision is likely to cause a mismatch between nebulin and its thin filament binding sites, possibly promoting degradation of nebulin's N-terminus. Thus, the reduced immunoreactivity of nebulin's N-terminus is consistent with heightened vulnerability of nebulin's N-terminal region. To study nebulin protein levels, we used SDS–PAGE on five NM-NEB patients and four controls. As shown in Figure 2B and C, control quadriceps shows a clear nebulin band at $\sim$800 kDa, with an expression level of 0.08 ± 0.01 (nebulin/myosin ratio). SDS–PAGE showed that nebulin in NM-NEB patients has a mobility that is indistinguishable from that of controls, which is expected because exon 55 represents only 4 kDa at the protein level, far below the detection limit of proteins in the (near) mega Dalton weight range. Importantly, gel analysis indicated significantly reduced nebulin levels, from $\sim$0.08 in controls to 0.01 ± 0.01 (nebulin/myosin ratio) in NM-NEB muscle (Fig. 2C). A large reduction in nebulin content has also been noted in other NM patients with nebulin mutations (14), and might be due to an increase in nebulin's vulnerability to proteolysis that results from a lower binding affinity of mutant nebulin for the thin filament. In summary, muscle of NM-NEB patients has greatly reduced nebulin protein levels, with the most prominent reduction at nebulin's N-terminal end.

Altered force–sarcomere length relations in NM-NEB muscle suggest shorter and non-uniform thin filaments

Previous work with a nebulin knockout mouse model has shown that nebulin regulates thin filament length (6,7): nebulin-deficient skeletal muscle exhibited shorter thin filaments (6,7), that might become non-uniform in length during muscle loading (6,8). Because sarcomeres generate force in proportion to thick and thin filament overlap, a well-defined thin filament length is an important determinant of proper muscle function. This is illustrated by the force–sarcomere length relation, which is characterized by a force plateau at optimal filament overlap, followed by a descending limb at higher sarcomere lengths as filament overlap decreases. Shortened thin filaments will reduce thick and thin filament overlap and impair the sarcomere's force generating capacity, which is reflected by a leftward shift of the force–sarcomere length relation. In addition, no optimal overlap exists when sarcomeres contain non-uniform thin filament lengths, and the force–sarcomere length

relation will not have a plateau. Hence, we studied whether the significantly reduced nebulin levels in skeletal muscle of NM-NEB patients affects thin filament length regulation, and muscle force generating capacity. We used skinned fiber preparations to determine the force–sarcomere length relations of NM-NEB and control skeletal muscle. To examine the similarity between nebulin-deficient mouse muscle and human NM-NEB muscle, we provide a side-by-side comparison of results obtained with NM-NEB muscle and data from the nebulin KO mouse model. As the KO mice typically die within 1–2 weeks after birth most likely due to respiratory failure (6), the mice used for the present study were between 8 and 10 days old.

We first determined the force–sarcomere length relation of slow- and fast-type fibers. Consistent with the clinical pathology reports on several of these biopsies, our SDS–PAGE analysis for myosin isoforms in NM-NEB muscles revealed only slow-type muscle fibers (Fig. 3A, right), whereas control quadriceps contained both slow-type and fast-type fibers (it has not been investigated in human fibers whether force–sarcomere length relations are fiber-type dependent). Single muscle fibers were skinned and the force in response to saturating [Ca^{2+}] was determined at various sarcomere lengths. Subsequently, the fibers were typed using SDS–PAGE. The resulting force–sarcomere length relation for slow-and fast-type fibers from controls overlap, as shown in Figure 3A, indicating that force–sarcomere length relations are fiber-type independent.

Next, we obtained force–sarcomere length relations of skinned fiber preparations isolated from control as well as NM-NEB muscle. Control fibers showed a characteristic force plateau up to $\sim$2.8 μm, followed by a linear descending limb (Fig. 3B). Thus, these functional data show that control muscle thin filaments are of a uniform and well-defined length. Note that the descending limb of control fibers intercepts the x-axis at $\sim$4.2 μm. Assuming that thick filaments are constant at $\sim$1.6 μm (15), this would suggest that thin filament length is $\sim$1.3 μm (these data are in line with thin filament lengths as determined by our IF and EM studies, see in what follows). Importantly, fibers from NM-NEB patients showed a leftward-shift of the force–sarcomere length relation, indicating shorter thin filament lengths (Fig. 3B). Furthermore, the force plateau, characteristic for uniform thin filament lengths, was absent in NM-NEB fibers suggesting that thin filament lengths of NM-NEB muscle are not only shorter, but also non-uniform (It should be noted that in theory a force plateau could be present in NM-NEB fibers at sarcomere lengths shorter than 2.0 μm, but unfortunately at these lengths the striation pattern of the fibers became unclear, precluding the reliable determination of sarcomere length). Considering that thin filament length is an important determinant of a muscle's force generating capacity, we also plotted stress [force normalized to fiber cross-sectional area (CSA)] generated by control and NM-NEB fibers versus sarcomere length. Control fibers generated maximal stress at 2.8 μm sarcomere length, whereas NM-NEB at 2.0 μm. Importantly, maximal stress was greatly reduced ($\sim$65%) in fibers from NM-NEB patients compared with control fibers (Fig. 3B, right). The force–sarcomere length relation of NebKO muscle showed similar features as NM-NEB muscle (Fig. 3C), and maximal stress of NebKO muscle was decreased more than 50% as well. It should be noted that, in addition to thin filament characteristics, myofibrillar disarray is expected to also contribute to the reduced maximal stress in NM-NEB patients. However, the shift in the force–sarcomere length relation and absence of a plateau is likely solely due to altered thin filament lengths. Thus, our force–sarcomere length relation data suggest that skeletal muscle of NM-NEB patients have shorter and non-uniform thin filament lengths compared with control muscle. This likely contributes to the significantly impaired force generating capacity of skeletal muscle in these patients.

Structural studies

We investigated thin filament length using immunofluorescence confocal scanning laser microscopy (IF) and electron microscopy (EM). We first localized tropomodulin, a thin filament pointed-end capping protein that has been used by others as a determinant of thin filament length (7,16). In control myofibrils tropomodulin staining showed a distinct doublet in the middle of the sarcomere, 2.75 ± 0.01 μm apart (measured across the Z-disk, Fig. 4A), indicating that thin filament lengths are uniform and $\sim$1.35 μm long (note that the force–sarcomere length relation yielded approximately similar thin filament length data for controls, Fig. 3B). However, in myofibrils from NM-NEB patients tropomodulin staining revealed a single broad and indistinct band centered over the Z bands. Alpha-actinin (a Z-disk marker) staining showed regular striation patterns (Fig. 4A and B) indicating well-organized myofibrillar structure. In NM-NEB myofibrils tropomodulin had translocated towards the Z-disk and densitometry analysis showed that this near-Z-disk zone had a width (measured at half-maximal intensity) of 1.55 ± 0.36 μm (Fig. 4A, right). These findings suggest that thin filament lengths in NM-NEB myofibrils are significantly shorter and non-uniform (because of the broad staining region). The tropomodulin staining pattern in myofibrils from NebKO mice showed striking similarity with the tropomodulin staining of NM-NEB myofibrils: absence of the doublet in the middle of the sarcomere, but instead translocation towards the Z-disk (Fig. 4B). Note that in control and wt myofibrils the anti-tropomodulin antibody weakly stained the Z-disk. This has been observed previously in studies using this antibody (6) and is considered non-specific binding to an unknown z-disk component. In summary, in NM-NEB myofibrils the thin filament capping protein tropomodulin is translocated towards the Z-disk, suggesting shorter and non-uniform thin filament lengths.

IF studies with fluorescently labeled phalloidin (which binds filamentous actin with high affinity) were also carried out. The labeling patterns of myofibrils from NM-NEB patients and controls differed remarkably: controls showed broad actin labeling with uniform intensity (except for the Z-disk area), whereas in NM-NEB myofibrils the labeling was narrower, and intensity gradually decreased from the Z-disk towards the middle of the sarcomere (Fig. 4C). Densitometric analysis revealed that the width at half-maximal intensity was 2.45 ± 0.01 μm for controls and 1.46 ± 0.11 μm for NM-NEB myofibrils (Fig. 4C, right). Thus, in line with the tropomodulin data, our phalloidin studies indicate significant shorter and non-uniform thin filament lengths in NM-NEB myofibrils. Actin staining of NM-NEB myofibrils was similar to that of NebKO myofibrils (Fig. 4D).

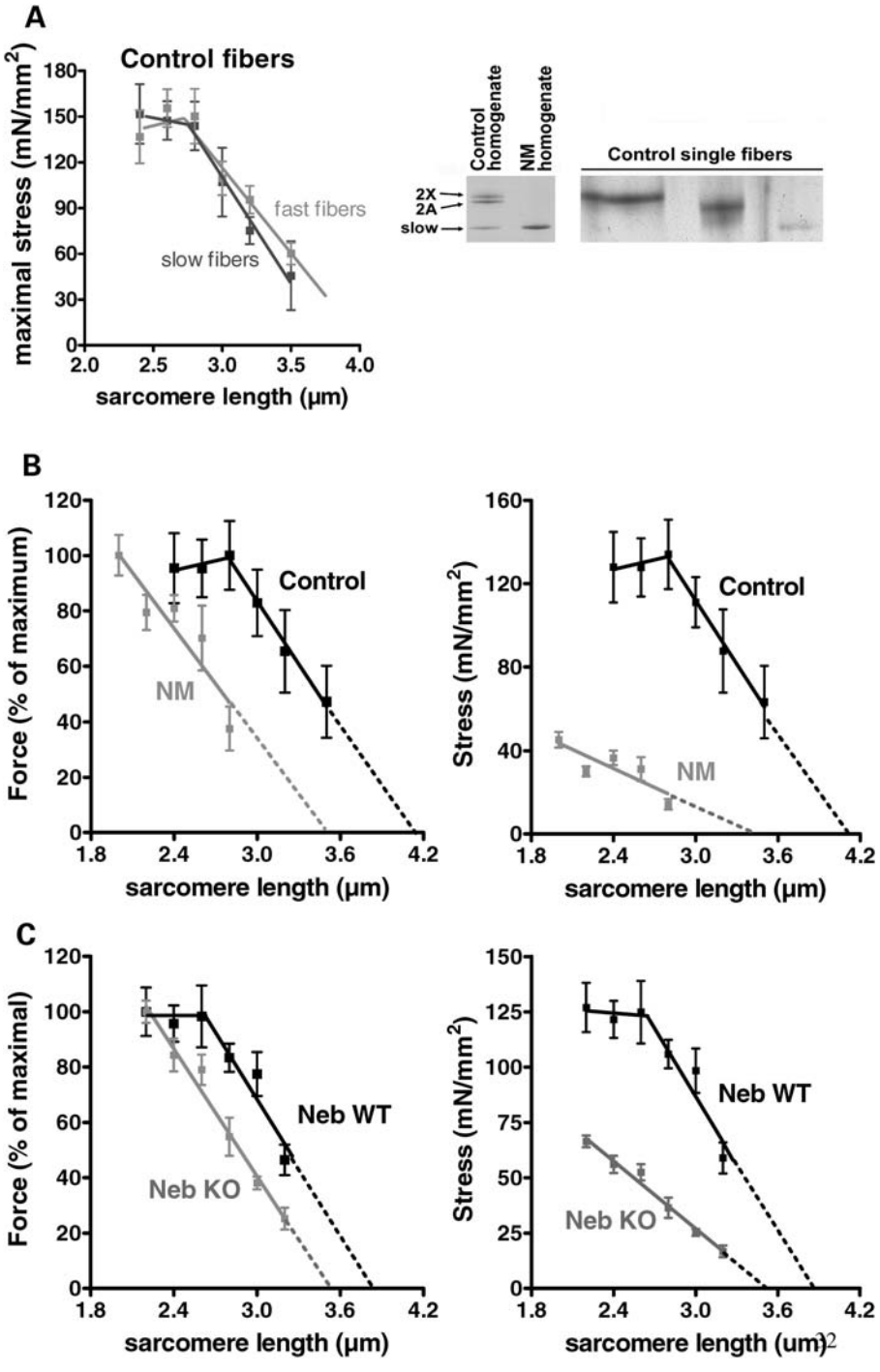

Figure 3. (**A**) Left: Force–sarcomere length relation of control fibers expressing slow and fast isoforms of myosin heavy chain. Right: SDS–PAGE of muscle homogenates from controls reveal expression of slow and fast (2A, and 2X) myosin heavy chain isoforms. NM-NEB homogenates contain only slow isoforms of myosin heavy chain. The majority of single fibers isolated from control biopsies expressed only a single myosin heavy chain isoform. (**B**) Left: The force–sarcomere length relation of control fibers has a characteristic force plateau followed by a descending limb. The force–sarcomere length relation of NM-NEB fibers is shifted leftward compared with control fibers, and the force plateau is absent. Right: Plotting stress (force normalized to fiber CSA) versus sarcomere length illustrates >65% reduction in stress generating capacity in NM fibers. (**C**) The force–sarcomere length relation of NebKO muscle is also shifted to the left (as found for NM fibers in B). Maximal stress is more than 50% reduced in NebKO compared with wt muscle. Data are based on ∼50 fibers per group.

EM showed overall normal sarcomeric structure in NM-NEB myofibrils, although Z-disks appeared wider in NM-NEB myofibrils. Because α-actinin staining appeared wider as well in NM-NEB compared with control myofibrils (Fig. 4A), and previous work revealed Z-disk widening in NebKO muscle (6), we performed Z-disk width measurements using EM micrographs. These analyses revealed that the majority of Z-disks in control myofibrils from quadriceps muscle have a width of

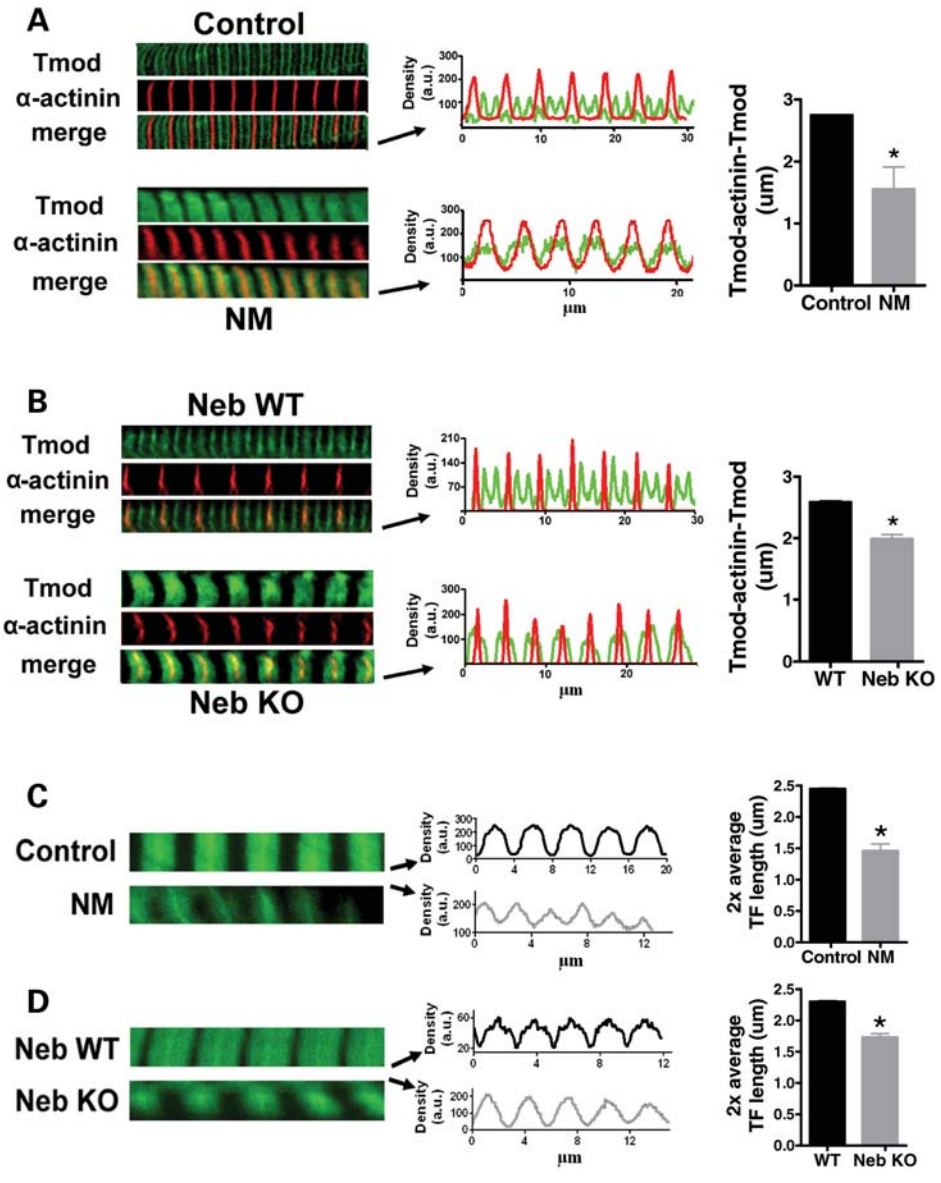

Figure 4. (**A**) Myofibrils from controls and NM-NEB patients stained for α-actinin and tropomodulin (Tmod). Left: Note the tropomodulin doublet in the middle of the sarcomere in control myofibrils, but diffuse staining in NM-NEB myofibrils. Middle: overlay of line scan intensity profile of α-actinin and tropomodulin. Right: The distance between tropomodulin staining (measured across the Z-disk, and indicated as Tmod-α-actinin-Tmod) is significantly reduced in NM-NEB myofibrils. (**B**) Alpha-actinin and tropomodulin staining of NebKO myofibrils is similar to the staining pattern of NM-NEB myofibrils in (A). (**C**) Left: Actin staining with phalloidin shows broad and homogenous staining in control myofibrils, whereas actin staining intensity in NM-NEB myofibrils gradually decreases from Z-disk towards the middle of the sarcomere. Middle and right: Analysis of phalloidin line scan intensities revealed significantly reduced average thin filament (TF) lengths in NM-NEB myofibrils. (**D**) Actin staining of NebKO myofibrils shows high resemblance with staining of NM myofibrils shown in (C). Data are based on ∼15 fibers per group.

either ∼70 or ∼101 nm. Quadriceps is a mixed muscle type containing both slow- and fast-type muscle fibers, and it is well established that Z-disks are wider in slow-type fibers (17). Thus, most likely the average Z-disk width in myofibrils from fast-type muscle fibers is ∼70 versus ∼100 nm for Z-disks from slow-type fibers (which is in line with previous reports) (17). NM-NEB quadriceps expresses only slow-type muscle fibers (see Fig. 3A); however, Z-disk width in NM-NEB myofibrils averaged ∼120 nm, rather than the ∼100 nm found in slow-type control myofibrils. These findings are in line with the notion that when nebulin is absent or reduced, regulation of Z-disk width is compromised (6). In addition to these changes in Z-disk width, a consistent finding was that control sarcomeres had a distinct H-zone (i.e. thin filament bare zone in the middle of the sarcomere, Fig. 5A top), and this feature was absent in NM-NEB sarcomeres (Fig. 5A bottom). For these experiments sarcomeres were stretched to ∼2.9 μm (as in Fig. 5A). Considering that at 2.9 μm NM-NEB sarcomeres still produce ∼40% of maximal force (Fig. 3B), absence of the H-zone at this sarcomere length cannot be explained by complete loss of thin and thick filaments overlap. To verify that the number of thin filaments was not

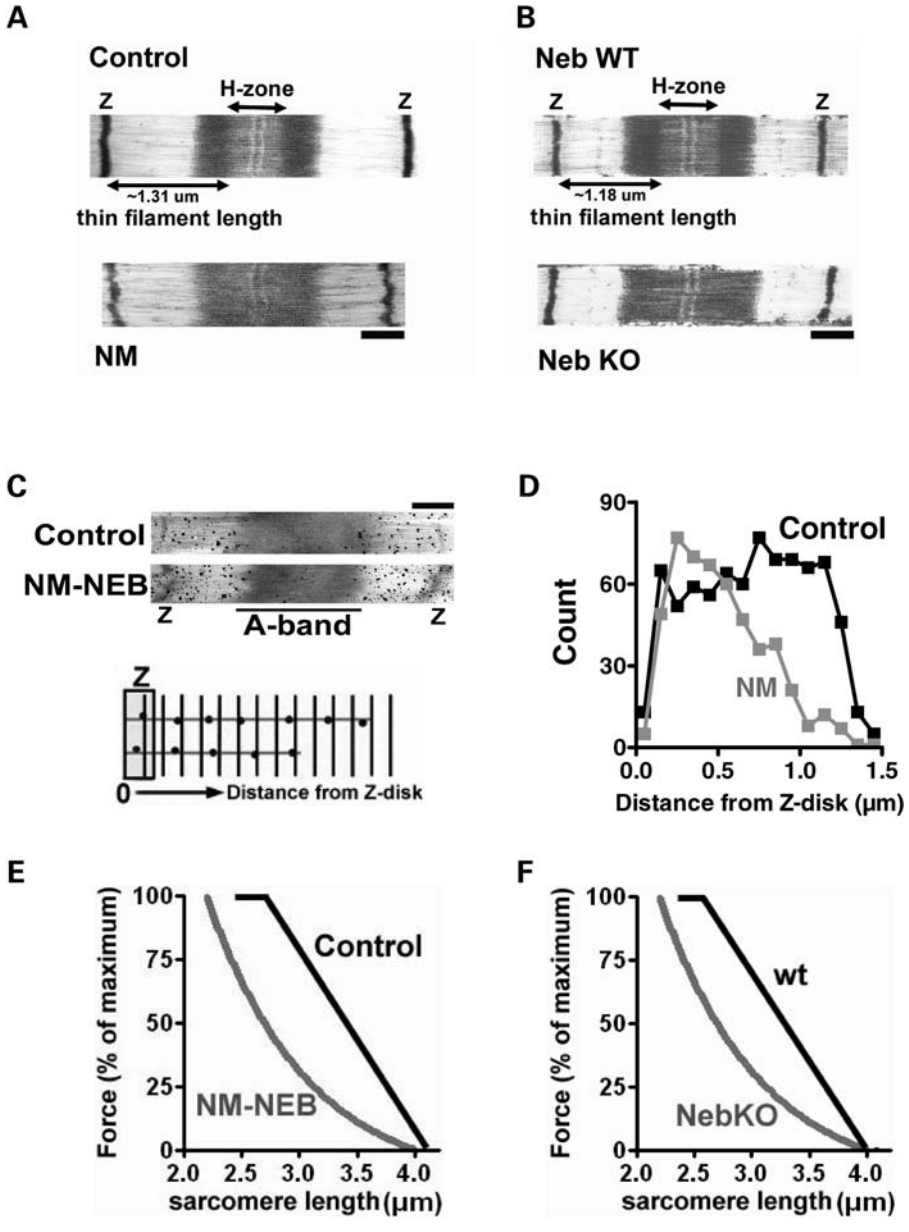

Figure 5. (**A**) Electron micrograph of control and NM-NEB myofibrils. Note that the H-zone (thin filament devoid zone) is only visible in control sarcomeres. (**B**) Similar findings were obtained in NebKO myofibrils. (**C**) Control and NM-NEB myofibrils labeled with phalloidin-biotin, followed by streptavidin-nanogold and silver enhancement (Bars: 0.5 μm). Bottom: Schematic showing how the distance between silver grains and the Z-disk was defined. (**D**) Histograms of obtained distances for control and NM-NEB myofibrils. Results suggest that in NM-NEB myofibrils thin filaments vary in length between ∼0.4 and ∼1.3 μm. (**E**) Predicted force–sarcomere length relations for control and NM-NEB muscle, assuming that thin filament length in NM-NEB muscle varies between ∼0.4 and 1.3 μm, and is uniform in control muscle at ∼1.3 μm. Note the leftward shift of the predicted force–sarcomere length relation and the absence of a force plateau in NM-NEB muscle. (**F**) The predicted force–sarcomere length relation of wt and NebKO muscle (based on previously published phalloidin labeling patterns) (6). The shift of the NebKO muscle is similar to that of NM-NEB fibers.

reduced in NM-NEB myofibrils (which could make it more difficult to identify a distinct H-zone), we made cross-sections and measured thin filament density near the Z-disk where the thin filaments are organized in a square-like pattern (total number of filaments represented in the measurements: 1457 for control and 1511 for NM samples, measurements performed at a sarcomere length of ∼2.9 μm). According to our measurements, the number of thin filaments per unit area was comparable between control and NM-NEB myofibrils (3428 ± 114 versus 3262 ± 111 thin filaments/μm^2, control versus NM-NEB, respectively, $P = 0.3$). We also performed an SDS–PAGE analysis of actin-myosin ratios and found this ratio to be reduced in NM-NEB samples relative to control fibers to $63 \pm 8\%$ ($n = 4$; $P = 0.03$). Thus, these data support the notion that the absence of a distinct H-zone in NM-NEB sarcomeres is not caused by a reduction in the number of thin filaments in NM-NEB muscle, but rather due to thin filaments being shorter and non-uniform in length. NebKO sarcomeres showed

absence of a distinct H-zone as well, again displaying great similarity with NM-NEB muscle, as shown in Figure 5B.

Finally, we labeled skinned muscle fibers with phalloidin conjugated to biotin, followed by streptavidin-coated gold beads that were silver-enhanced. Then, by measuring the distance of the silver grains to the Z-disk (see Fig. 5C bottom for schematic) and plotting results in a histogram, thin filament length can be assessed. These experiments allow thin filament length distributions to be determined with high resolution. It should be noted however, that the power of this method comes from analysis of a large number of sarcomeres. In general, data from a single sarcomere (as shown in Fig. 5C) are not conclusive, whereas extensive analyses of many sarcomeres can reveal differences in thin filament length distributions between control and NM-NEB. Thus, by analyzing a large set of sarcomeres valuable insights can be obtained. We found that in control myofibrils, the silver grains were evenly distributed up to $\sim$1.3 μm from the Z-disk (Fig. 5D). In contrast, grain distribution in NM-NEB myofibrils indicates that thin filaments are shorter and non-uniform in length, ranging from $\sim$0.3 to $\sim$1.3 μm (Fig. 5D). Using this thin filament range, and assuming that all intermediate thin filament lengths are equally represented (Fig. 5D shows that this is likely correct), we derived a predicted force–sarcomere length relation for control and NM-NEB muscle. Note that the predicted force–sarcomere length relation of NM-NEB muscle is shifted to the left, and that a force plateau is only predicted for control muscle (Fig. 5E). Figure 5F shows the predicted force–sarcomere length relation of NebKO muscle, based on previously published phalloidin labeling patterns (6). Importantly, the predicted force–sarcomere length relations of NM-NEB and NebKO both show striking similarity to the *measured* force–sarcomere length relations shown in Figure 3B and C. Thus, these results further support that thin filaments are of a well-defined length in control muscle, but are shorter and of non-uniform length in NM-NEB muscle, thereby affecting the muscle's force generating capacity.

DISCUSSION

While recent studies on nebulin-free murine myofibrils revealed impaired contractility, the pathogenesis of muscle weakness in patients with NM has remained obscure, in part because of genetic heterogeneity and difficulty in obtaining well preserved and genetically characterized biopsies. Here, we have studied patients with NM caused by a homozygous deletion of nebulin's exon 55, causing a partial knockdown of the remaining internally truncated nebulin. The side-by-side comparison of partial nebulin-deficient human myofibrils with nebulin-free murine myofibrils indicates shorter and non-uniform thin filament lengths as well as severe muscle weakness as a common phenotype.

Deletion of nebulin exon 55 in patients with NM

Nebulin is encoded by a single gene containing 183 exons in humans (18). Approximately ninety-seven of these exons are 100–120 bp in length and code for a highly modular structure, the so-called SDXXYK-repeats (see Fig. 1B). A total of 185 SDXXYK repeats have been identified in the human nebulin mRNA (M1–M185); additional repeats were identified in the human and murine genomic sequences (18,19). Nebulin's N-terminal modules (M1–M8) contain binding sites for the thin filament pointed-end capping protein tropomodulin, and modules M163 through M185 are located in and near the Z-disk. The centrally located modules, M9–M162, are each thought to represent individual actin-binding motifs, and are organized into seven-module super-repeats that match the repeat of the actin filament (see Fig. 1B). This precise arrangement is thought to allow each nebulin module to interact with a single monomer of the actin filament (12,13).

Although mutations in six different genes have been implicated in NM, mutations in the nebulin gene are the most common cause of NM (4). Nebulin's large size has greatly hindered the identification of NM-causative mutations in the nebulin gene. Although to date many of the human *NEB* mutations are predicted to introduce nonsense codons or frame shifts (20), there are no proven 'nebulin null' patients, and this situation may in fact be a lethal condition in humans. Instead, virtually all NM patients appear to produce at least some truncated or internally deleted nebulin molecules, presumably due to an extensive and complex pattern of alternative splicing (4,21). Recently the first large NM-causing nebulin mutation has been discovered, i.e. deletion of exon 55 (carrier frequency $\sim$1 in 108 among Ashkenazi Jews) (22). Nebulin exon 55 codes for 35 amino acids that are part of modules M69 and M70 of the ninth super-repeat (Fig. 1B). This in-frame deletion of exon 55 likely causes a mismatch between nebulin and its actin binding sites, thereby reducing binding between nebulin and the thin filament. This has been speculated to increase nebulin's vulnerability to proteolysis (22). Indeed, our gel electrophoresis studies indicate an approximately 8-fold reduction of nebulin protein levels in skeletal muscle of NM-NEB patients. Furthermore, our western blot studies suggest that the reduced nebulin level is most prominent at nebulin's N-terminal end. We speculate that this is due to exon 55 being in closer proximity to nebulin's N-terminus than to its C-terminal end.

Deletion of nebulin exon 55 dysregulates thin filament length control and causes muscle fiber weakness in patients with NM

A hallmark feature of patients with NM is muscle weakness, greatly affecting daily life-activities and negatively impacting the quality of life (23). At the muscle structure level, NM is characterized by myofibrillar disarray originating from the Z-disk and culminating in nemaline rods, which consist of thin filament and Z-disk proteins (1,3,23). Importantly, the number of nemaline rods in muscle biopsies does not correlate with the muscle weakness observed in patients with NM (24,25). This suggests that myofibrillar disarray and nemaline rods are a secondary phenomenon and are not the sole contributors to the muscle weakness associated with NM. Our data provide evidence for the notion that reduced nebulin expression contributes to muscle weakness in NM-NEB patients, through loss of thin filament length regulation.

In skeletal muscle, thin filament lengths are fine tuned at $\sim$1.1–1.3 μm (depending on species and muscle type) (8) to overlap with thick filaments and to meet the muscle's

physiological requirements (8,26). The extent of overlap between thick and thin filaments determines the sarcomere's force generating capacity: short thin-filaments reduce overlap and impair force generation. Thus, thin filament length is a key aspect of muscle function. Since length is not an intrinsic property of actin filaments (actin monomers assemble *in vitro* and *in vivo* to many allowed polymer lengths) (27), their lengths are likely to be specified by an actin binding protein. Recent work indicates that nebulin acts as a ruler molecule that regulates thin filament length in skeletal muscle (6,7). This finding prompted us to examine the role of thin filament length regulation in the pathophysiology of muscle weakness in patients with NM due to nebulin mutations. First, functional studies revealed dramatic loss of force generating capacity in fibers from NM-NEB patients with nebulin exon 55 deletion (Fig. 3B, right). It is well established that muscle fibers from patients with NM undergo atrophy (25) resulting in fibers with smaller CSA, negatively impacting force production. Thus, an important finding of the present study was that force generation, even when normalized to fiber CSA, was more than 65% reduced in NM-NEB compared with controls. This suggests that intrinsic abnormalities at the myofilament level significantly contribute to muscle weakness in NM-NEB. To examine whether loss of thin filament length control is involved, we determined force–sarcomere length relations and found a leftward shift of the force–sarcomere length relation in skinned muscle fibers from NM-NEB patients (Fig. 3B), indeed indicating shorter thin filaments. Furthermore, the force plateau that is characteristic for uniform thin filament lengths (see Fig. 3B, control fibers), is absent in NM-NEB muscle fibers, suggesting that resulting thin filaments are not only shorter, but also non-uniform in length. A role for reduced thin filament length in NM-associated muscle weakness was further supported by electron microscopy studies with the actin-binding protein phalloidin. From these studies we derived the range of thin filament lengths present in control and NM-NEB myofibrils (Fig. 5B), which allowed us to predict the force–sarcomere length relation for control and NM fibers. As shown in Figure 5B, the predicted force–sarcomere length relation for NM-NEB muscle fibers shows remarkable resemblance with the measured force–sarcomere length relation (Fig. 3B). Furthermore, the thin filament length distribution present in control and NM-NEB myofibrils allowed us to predict to what extent thin filament length changes in NM-NEB myofibrils contribute to muscle weakness in these patients. We calculated thin–thick filament overlap in NM-NEB and control myofibrils at a sarcomere length of 2.2 μm assuming that thin filament lengths in NM-NEB myofibrils range from 0.3 to 1.3 μm and are a constant 1.3 μm in controls (Fig. 5D). According to this calculation thin filament length reduction is predicted to reduce thick–thin filament overlap, and thus force production, by ∼37% in NM-NEB myofibrils, which is about half of the total force reduction of ∼65% (Fig. 3B). Thus, the combination of our functional, ultrastructural and immunofluorescence studies, all support that average thin filament length is reduced from ∼1.3 μm in control muscle to ∼0.75 μm in muscle from NM patients with nebulin exon 55 deletion, significantly contributing to the muscle weakness observed in these patients.

Studies with nebulin-deficient skeletal muscle show striking similarity with NM-NEB muscle

The combination of studies on muscle fibers from NM-NEB patients, and nebulin-deficient mouse muscle provided us with a unique tool to test whether the functional and structural alterations observed in NM fibers are a direct effect of nebulin-deficiency or a secondary myopathic effect. As shown in Figures 3–5, the functional characteristics and (ultra)structure of fibers from NM-NEB patients show striking similarity with those of nebulin-deficient mouse fibers. As suggested previously (6,7), and confirmed by our extended studies on contractile function, nebulin-deficient mouse muscle displays >50% reduced maximal force generating capacity (normalized to fiber CSA) compared with wt muscle, accompanied by a leftward shift of the force–sarcomere length relationship. The structural studies on nebulin-deficient mouse muscle support these findings and suggest a reduction of thin filament length from ∼1.2 μm in wt muscle to an average of ∼0.85 μm in nebulin-deficient muscle. It should be noted that the NebKO mice are growth retarded at the age of 8–10 days after birth (6). Although we cannot rule out that growth retardation contributes to the thin filament length changes found in nebulin-deficient muscle, so far no data are available suggesting that thin filaments become longer and more uniform in length during muscle development. Thus, the marked similarity between the phenotypes of nebulin-deficient mouse muscle and NM-NEB muscle supports an important role for nebulin and loss of thin filament length regulation in the pathogenesis of muscle weakness in these patients.

Clinical relevance

Although muscle weakness is considered a hallmark feature of NM, its pathogenesis is poorly understood. The present study is the first to show a distinct genotype-functional phenotype correlation in patients with NM due to a nebulin mutation, and provides evidence for the notion that dysregulated thin filament length is an important contributor to muscle weakness in NM patients with nebulin mutations. Considering that nebulin mutations are the main cause of NM, these findings provide important insight into the pathophysiology of muscle weakness in NM patients.

Based on the present study, we expect that in patients with NM due to nebulin mutations muscle weakness is predominant at longer muscle lengths. In line with this expectation, previous work examining the force–knee–angle relation of quadriceps muscle during *in vivo* muscle contractions in patients with NM revealed that quadriceps muscle weakness was most prominent at higher knee flexion angles, i.e. at longer muscle lengths (28). Unfortunately, the disease causing gene mutations in these patients were not known. However, since nebulin mutations account for ∼50% of NM cases, it is likely that at least some of the examined patients harbored nebulin mutations. Insights in the effect of shorter thin filaments on force production can only be fully evaluated by knowing the *in vivo* sarcomere length range of control and NM patients with nebulin mutations and future studies should be directed at establishing this range. Although speculative, one mechanism by which muscle weakness induced by thin filament length changes in NM patients

might be alleviated could be by having muscles operate at shorter sarcomere lengths (by increasing the number of sarcomeres in series), and thereby increasing thin–thick filament overlap.

So far, there has been a lack of treatment regimens that counteract NM-associated muscle weakness, mainly due to a poor understanding of its pathophysiology. Thus, more research is needed to elucidate the muscle contractile phenotype of NM patients with different gene mutations. Knowledge of genotype-functional phenotype correlations could open therapeutic windows for treatment regimens specified to the gene mutation involved.

MATERIALS AND METHODS

Muscle biopsies from NM patients

Surgically obtained skeletal muscle specimens, remaining from diagnostic procedures or obtained during clinically indicated surgical procedures, were collected from five NM and four unaffected control patients following informed consent supervised by the Children's Hospital Boston IRB, and stored frozen and unfixed at −80°C until use (Table 1). All five Ashkenazi Jewish NM patients with deletion of *NEB* exon 55 have been reported previously and have been shown to carry identical homozygous deletion mutations as determined by both deletion and haplotype analysis (10).

Western blotting and gel electrophoresis

For nebulin expression, muscle samples were homogenized and analyzed on 2.6–7% SDS–acrylamide gels (29). Gels were scanned and analyzed with One-D scan EX (Scanalytics Inc., Rockville, MD, USA) software. The integrated optical density of nebulin and myosin heavy chain (MHC) was determined. For western blot analysis of nebulin epitopes, antibodies against nebulin N-terminus, nebulin C-terminus and nebulin serine-rich domain were used (6). For myosin heavy chain isoform composition, skeletal muscles were denatured by boiling for 2 min. The stacking gel contained a 4% acrylamide concentration (pH 6.7), and the separating gel contained 7% acrylamide (pH 8.7) with 30% glycerol (v/v). The gels were run for 24 h at 15°C and a constant voltage of 275V. Finally, the gels were silver-stained, scanned and analyzed with One-D scan EX software. For myosin heavy chain isoform composition of single fibers used for muscle mechanics, fibers were detached from the force transducer and servo-motor and processed as described earlier.

Muscle contractility experiments

The procedures for skinned muscle contractility were as described previously (30,31), with minor modifications. In short, small strips dissected from muscle biopsies were skinned overnight at ∼4°C in relaxing solution (in mM; 20 BES, 10 EGTA, 6.56 $MgCl_2$, 5.88 NaATP, 1 DTT, 46.35 K-propionate, 15 creatine phosphate, pH 7.0 at 20°C) containing 1% (v/v) Triton X-100. The skinning procedure renders the membranous structures in the muscle fibers permeable, which enables activation of the myofilaments with exogenous Ca^{2+}. Preparations were washed thoroughly with relaxing solution and stored in 50% glycerol/relaxing solution at −20°C. Small muscle bundles (diameter ∼0.07 mm) were dissected from the skinned strips, and were attached to a strain gauge and a high-speed motor using aluminium foil clips. Experiments were performed at 20°C. The XY (width) and XZ (depth, using a prism) bundle diameters were measured with a ×40 objective. The muscle bundle CSA was calculated from the average of three width and depth measurements made along the length of the muscle bundle. The preparation was activated at pCa 4.5 to obtain maximal Ca^{2+}-activated force. Maximal stress was determined by dividing the force generated at pCa 4.5 by CSA. To determine force–sarcomere length relations, the maximal force generated at various sarcomere lengths was determined. Sarcomere length was measured with an online laser-diffraction system (32).

Immunofluorescence confocal scanning laser microscopy and electron microscopy

Small strips were dissected from the biopsies and skinned overnight at ∼4°C in relaxing solution (in mM; 20 BES, 10 EGTA, 6.56 $MgCl_2$, 5.88 NaATP, 1 DTT, 46.35 K-propionate, 15 creatine phosphate, pH 7.0 at 20°C) containing 1% (v/v) Triton X-100. Immuno-labeling and confocal scanning laser microscopy was performed essentially as described previously (6). Primary antibodies: anti-α-actinin (mouse monoclonal, A7811, Sigma-Aldrich), anti-tropomodulin-1 (6) and Alexa Fluor 488 conjugated phalloidin (A12379, Invitrogen). Secondary antibodies: Alexa Fluor 594 (goat anti-mouse, Invitrogen) and Alexa Fluor 488 (goat anti-rabbit, Invitrogen). Secondary antibodies did not stain when used without primary antibodies (data not shown). Images were produced using a Bio-Rad MRC 1024 confocal laser scanning microscope using the LaserSHARP 2000 software package (Hercules, CA, USA). From the acquired images, thin filament lengths were determined using ImageJ software (National Institutes of Health).

For electron microscopy, small muscle bundles were dissected, and skinned overnight as described earlier. Subsequently, skinned bundles were fixed in 3.7% paraformaldehyde, and labeled overnight with phalloidin-biotin (B7474, biotin-XX phalloidin, Invitrogen), followed by streptavidin-nanogold (#2016, nanogold streptavidin conjugate, Nanoprobes), silver enhancement as per instructions with Nanogold HQ silver kitfixing and embedding. EM was performed as previously described (6). For determination of thin filament density, fibers were cross-sectioned (75 nm thick sections stained with uranyl acetate and lead citrate) and then longitudinally for sarcomere length measurements.

Nebulin knockout mouse model

The nebulin knockout mouse model has been described previously (6). In brief, destruction of the TATA motif and murine nebulin exon 1 including the start ATG was achieved by homologous recombination. Three mouse lines were raised from independent ES-cell clones. KO mice typically die within ∼10 days after birth due to severe muscle weakness resulting in respiratory failure and mice used for the present study were between 8 and 10 days old. All animal experiments were approved by IACUC and followed the NIH Guidelines

'Using Animals in Intramural Research' for animal use. Protein analysis studies, muscle contractile performance studies, immunofluorescence studies and electron microscopy studies were performed as described earlier.

Statistical analysis

The data are presented as means $\pm$ SEM. Statistical analyses were performed by *t*-test; $P < 0.05$ was considered statistically significant.

ACKNOWLEDGEMENTS

We thank Ms Tiffany Pecor and Mr Mark McNabb for outstanding technical assistance, and Elizabeth DeChene MS for assistance collecting and characterizing muscle biopsies.

Conflict of Interest statement. None declared.

FUNDING

This work was supported by a VENI grant from the Dutch Organization for Scientific Research to C.A.C.O., by the DFG [to C.C.W. (Wi3278/1-1)], by National Institutes of Health (AR053897 to H.G., AR044345 to A.H.B.] and the Lee and Penny Anderson Family Foundation and the Joshua Frase Foundation to A.H.B.

REFERENCES

1. Morris, E.P., Nneji, G. and Squire, J.M. (1990) The three-dimensional structure of the nemaline rod Z-band. *J. Cell. Biol.*, **111**, 2961–2978.
2. Agrawal, P.B., Greenleaf, R.S., Tomczak, K.K., Lehtokari, V.L., Wallgren-Pettersson, C., Wallefeld, W., Laing, N.G., Darras, B.T., Maciver, S.K., Dormitzer, P.R. and Beggs, A.H. (2007) Nemaline myopathy with minicores caused by mutation of the CFL2 gene encoding the skeletal muscle actin-binding protein, cofilin-2. *Am. J. Hum. Genet.*, **80**, 162–167.
3. Sanoudou, D. and Beggs, A.H. (2001) Clinical and genetic heterogeneity in nemaline myopathy–a disease of skeletal muscle thin filaments. *Trends Mol. Med.*, **7**, 362–368.
4. Pelin, K., Hilpela, P., Donner, K., Sewry, C., Akkari, P.A., Wilton, S.D., Wattanasirichaigoon, D., Bang, M.L., Centner, T., Hanefeld, F. *et al.* (1999) Mutations in the nebulin gene associated with autosomal recessive nemaline myopathy. *Proc. Natl. Acad. Sci. USA*, **96**, 2305–2310.
5. Wang, K. and Wright, J. (1988) Architecture of the sarcomere matrix of skeletal muscle: immunoelectron microscopic evidence that suggests a set of parallel inextensible nebulin filaments anchored at the Z line. *J. Cell Biol.*, **107**, 2199–2212.
6. Witt, C.C., Burkart, C., Labeit, D., McNabb, M., Wu, Y., Granzier, H. and Labeit, S. (2006) Nebulin regulates thin filament length, contractility, and Z-disk structure in vivo. *EMBO J.*, **25**, 3843–3855.
7. Bang, M.L., Li, X., Littlefield, R., Bremner, S., Thor, A., Knowlton, K.U., Lieber, R.L. and Chen, J. (2006) Nebulin-deficient mice exhibit shorter thin filament lengths and reduced contractile function in skeletal muscle. *J. Cell Biol.*, **173**, 905–916.
8. Littlefield, R.S. and Fowler, V.M. (2008) Thin filament length regulation in striated muscle sarcomeres: Pointed-end dynamics go beyond a nebulin ruler. *Semin. Cell Dev. Biol.*, **19**, 511–519.
9. Huxley, A.F. and Simmons, R.M. (1971) Proposed mechanism of force generation in striated muscle. *Nature*, **233**, 533–538.
10. Lehtokari, V.L., Greenleaf, R.S., Dechene, E.T., Kellinsalmi, M., Pelin, K., Laing, N.G., Beggs, A.H. and Wallgren-Pettersson, C. (2009) The exon 55 deletion in the nebulin gene - One single founder mutation with world-wide occurrence. *Neuromuscul. Disord.*, **19**, 179–181.
11. Wang, K., Knipfer, M., Huang, Q.Q., van Heerden, A., Hsu, L.C., Gutierrez, G., Quian, X.L. and Stedman, H. (1996) Human skeletal muscle nebulin sequence encodes a blueprint for thin filament architecture. Sequence motifs and affinity profiles of tandem repeats and terminal SH3. *J. Biol. Chem.*, **271**, 4304–4314.
12. Labeit, S., Gibson, T., Lakey, A., Leonard, K., Zeviani, M., Knight, P., Wardale, J. and Trinick, J. (1991) Evidence that nebulin is a protein-ruler in muscle thin filaments. *FEBS Lett.*, **282**, 313–316.
13. Labeit, S. and Kolmerer, B. (1995) The complete primary structure of human nebulin and its correlation to muscle structure. *J. Mol. Biol.*, **248**, 308–315.
14. Gurgel-Giannetti, J., Reed, U., Bang, M.L., Pelin, K., Donner, K., Marie, S.K., Carvalho, M., Fireman, M.A., Zanoteli, E., Oliveira, A.S. *et al.* (2001) Nebulin expression in patients with nemaline myopathy. *Neuromuscul. Disord.*, **11**, 154–162.
15. Walker, S.M. and Schrodt, G.R. (1974) I segment lengths and thin filament periods in skeletal muscle fibers of the Rhesus monkey and the human. *Anat. Rec.*, **178**, 63–81.
16. Rajasekaran, M.R., Jiang, Y., Bhargava, V., Littlefield, R., Lee, A., Lieber, R.L. and Mittal, R.K. (2008) Length-tension relationship of the external anal sphincter muscle: implications for the anal canal function. *Am. J. Physiol. Gastrointest. Liver Physiol.*, **295**, G367–G373.
17. Engel, A.G. and Franzini-Armstrong, C. (2004) *Myology*, 3rd edn. McGraw-Hill Professional, New York, USA.
18. Donner, K., Sandbacka, M., Lehtokari, V.L., Wallgren-Pettersson, C. and Pelin, K. (2004) Complete genomic structure of the human nebulin gene and identification of alternatively spliced transcripts. *Eur. J. Hum. Genet.*, **12**, 744–751.
19. Kazmierski, S.T., Antin, P.B., Witt, C.C., Huebner, N., McElhinny, A.S., Labeit, S. and Gregorio, C.C. (2003) The complete mouse nebulin gene sequence and the identification of cardiac nebulin. *J. Mol. Biol.*, **328**, 835–846.
20. Lehtokari, V.L., Pelin, K., Sandbacka, M., Ranta, S., Donner, K., Muntoni, F., Sewry, C., Angelini, C., Bushby, K., Van den, B.P. *et al.* (2006) Identification of 45 novel mutations in the nebulin gene associated with autosomal recessive nemaline myopathy. *Hum. Mutat.*, **27**, 946–956.
21. Sewry, C.A., Brown, S.C., Pelin, K., Jungbluth, H., Wallgren-Pettersson, C., Labeit, S., Manzur, A. and Muntoni, F. (2001) Abnormalities in the expression of nebulin in chromosome-2 linked nemaline myopathy. *Neuromuscul. Disord.*, **11**, 146–153.
22. Anderson, S.L., Ekstein, J., Donnelly, M.C., Keefe, E.M., Toto, N.R., LeVoci, L.A. and Rubin, B.Y. (2004) Nemaline myopathy in the Ashkenazi Jewish population is caused by a deletion in the nebulin gene. *Hum. Genet.*, **115**, 185–190.
23. North, K.N., Laing, N.G. and Wallgren-Pettersson, C. (1997) Nemaline myopathy: current concepts. The ENMC International Consortium and Nemaline Myopathy. *J. Med. Genet.*, **34**, 705–713.
24. Shimomura, C. and Nonaka, I. (1989) Nemaline myopathy: comparative muscle histochemistry in the severe neonatal, moderate congenital, and adult-onset forms. *Pediatr. Neurol.*, **5**, 25–31.
25. Ryan, M.M., Ilkovski, B., Strickland, C.D., Schnell, C., Sanoudou, D., Midgett, C., Houston, R., Muirhead, D., Dennett, X., Shield, L.K. *et al.* (2003) Clinical course correlates poorly with muscle pathology in nemaline myopathy. *Neurology*, **60**, 665–673.
26. Burkholder, T.J., Fingado, B., Baron, S. and Lieber, R.L. (1994) Relationship between muscle fiber types and sizes and muscle architectural properties in the mouse hindlimb. *J Morphol.*, **221**, 177–190.
27. Pollard, T.D. and Borisy, G.G. (2003) Cellular motility driven by assembly and disassembly of actin filaments. *Cell*, **112**, 453–465.
28. Gerrits, K., Gommans, I., van Engelen, B. and de Haan, A. (2003) Quadriceps weakness in a family with nemaline myopathy: influence of knee angle. *Clin. Sci. (Lond)*, **105**, 585–589.
29. McCormick, K.M., Baldwin, K.M. and Schachat, F. (1994) Coordinate changes in C protein and myosin expression during skeletal muscle hypertrophy. *Am. J. Physiol.*, **267**, C443–C449.
30. Ottenheijm, C.A.C., Heunks, L.M., Geraedts, M.C. and Dekhuijzen, P.N. (2006) Hypoxia-induced skeletal muscle fiber dysfunction: role for reactive nitrogen species. *Am. J. Physiol. Lung Cell Mol. Physiol.*, **290**, L127–L135.
31. Ottenheijm, C.A., Fong, C., Vangheluwe, P., Wuytack, F., Babu, G.J., Periasamy, M., Witt, C.C., Labeit, S. and Granzier, H. (2008) Sarcoplasmic reticulum calcium uptake and speed of relaxation are depressed in nebulin-free skeletal muscle. *FASEB J.*, **22**, 2912–2919.
32. Granzier, H.L. and Wang, K. (1993) Interplay between passive tension and strong and weak binding cross-bridges in insect indirect flight muscle. A functional dissection by gelsolin-mediated thin filament removal. *J. Gen. Physiol.*, **101**, 235–270.